JOURNAL OF CATALYSIS 38, 1–10 (1975)

Structure and Catalytic Activity of $MoO_3 \cdot Al_2O_3$ Systems

III. Nature of Sites for Propylene Disproportionation

N. GIORDANO,[1] M. PADOVAN, A. VAGHI,
J. C. J. BART[2] AND A. CASTELLAN

Montedison, Research Centre of Bollate (Milano), Italy

Received April 3, 1974

The heterogeneous interaction of propylene with $MoO_3 \cdot \gamma Al_2O_3$ catalysts was studied by varying the composition and conditioning of the catalysts, and reaction parameters such as temperature and time. Catalysts activated at 500°C, containing up to 10–15 wt% MoO_3, exhibit disproportionation activity which is shown to be related to the presence of Mo(V) species originating from reduction of oxomolybdenum species. Evidence is presented indicating that dimeric Mo(V) configurations of bis-molybdenyl type are active in the reaction. This configuration appears to account for the formation of four-center complexes by bonding of olefin molecules in neighboring positions. Water negatively influences the disproportionation process.

INTRODUCTION

Catalysts based upon $MoO_3 \cdot Al_2O_3$ are remarkable for the multiplicity of the reactions they promote: these include polymerization and disproportionation of olefins, reforming of hydrocarbons, dehydrocyclization of *n*-paraffins, aldol condensation, dehydrogenation, H_2–D_2 exchange, hydrodesulfurization, and oxidation of olefins to ketones or acids. The body of results from all these investigations has concurred in indicating singularities in catalytic activity as a function of composition, thus justifying attempts to clear up relationships with solid state properties. In spite of considerable efforts in this direction there appear to be only a few examples in which solid state properties and catalytic behavior are closely related (*1–3*). This prompted us to undertake further investigations which started from a reconsideration of solid state properties of a series of impregnated and coprecipitated $MoO_3 \cdot Al_2O_3$ samples: extensive use of various techniques has led to considerable insight into the oxidized and reduced state, as discussed in Part I (*4*) and Part II (*5*) of this series.

Work along these lines has provided the basis for investigations on catalytic activity. By choosing propylene as a model reactant we have aimed at the determination of the sites on $MoO_3 \cdot Al_2O_3$ which are specific for the disproportionation to olefins and those specific for oxyhydration to acetone. The present article is devoted to the former reaction; it will be followed by Part IV (*6*) dealing with acetone formation.

EXPERIMENTAL METHODS

Apparatus and Experimental Procedure

Experiments to determine catalytic activity were carried out in a combined flow microreactor and gas chromatographic unit (Perkin-Elmer Model 154) under either pulse or tail conditions. A conventional microreactor of Pyrex glass

[1] Present address: Montedison Research Laboratories, Priolo (Sicily).

[2] Present address: Montedison Corporate Research Laboratories, Novara, Italy.

was used, with a stainless steel axial thermocouple and temperature regulation within ±2°C.

Samples will be referred to as indicated in Part I (*4*).

Pulse experiments were performed at 300°C using 0.25 g of the catalyst (42–65 mesh) and flow rates of helium of 40 cc/min. The volume of the pulse was 1.09 cc of propylene (99.5% purity). Particular care was given to the purification of He, by allowing it to flow through Anhydrone, molecular sieves and MnO traps, thus reducing the O_2 content to 2–3 ppm. To ensure quantitative comparison of catalytic performance, careful conditioning was found to be necessary; preliminary experiments showed that activity depended on the time and temperature of the *in situ* pretreatment. More drastic variations were observed in the case of samples with less than 10% MoO_3, probably due to more strongly chemisorbed water. Reproducible results were obtained by pretreating the catalysts at 500°C for 2–12 hr in a flow of He; subsequently, the samples were cooled down to 300°C. Pretreatment as above will be indicated as Mode 1. To emphasize the role of water, a slightly different procedure was adopted: samples pretreated as above were tested, also at $T = 300$°C, in the presence of water (2 μl) injected simultaneously with propylene (Mode 2).

Tail experiments were performed at temperatures in the 50 to 200°C range, using 4.5 cm^3 of catalyst (APS = 70 μm). MoO_3-10 samples were used throughout, as this composition was found to display maximum activity in pulse experiments. Flow rates of propylene were equivalent to contact times of 4 sec, as read at T and p of experiments. Catalysts, before use, were activated *in situ* in a stream of helium from which traces of water and O_2 had been removed in a series of purification traps consisting of Anhydrone and P_2O_5 for H_2O and MnO for O_2. Activation in helium was carried out at 540°C for 2 hr; afterwards, the catalyst was cooled to the reaction temperature in helium. Samples pretreated in this way will be designated "activated," as opposed to those designated "prereduced," which were prepared as above and then subjected to reduction by CO at 540°C for different periods of time (from 30 to 240 min), followed by cooling to reaction temperature, in helium. Spent catalysts were withdrawn from the microreactor in an inert atmosphere and sealed off in tubes for EPR analysis or analyzed by diffuse reflectance spectroscopy according to the procedure outlined previously (*5*).

Reactants and products were analyzed by a chromatographic unit using three different columns for separation of the various components. Characteristics of the columns are specified as follows:

Column A: stainless steel, 4 × 6 mm i.d., length 1.65 m; Ethofat (20%) and isophthalic acid (13%) on Gas-Chrom Cl (67%), for separation of acids (acetic, propionic, acrylic, in that order).

Column B: copper, 4 × 6 mm i.d., length 4 m; Carbowax 1500 (20%) on Chromosorb W leached with acids (80%), for separation of acetaldehyde, propylene oxide, propionaldehyde, acetone, acrolein, isopropyl alcohol, methylethylketone and benzene, in that order.

Column C: copper, 4 × 6 mm i.d., length 6.2 m; methylsulfolane (17%) on Chromosorb P leached with acids (87%), for separation of carbon monooxide, ethylene, carbon dioxide, propylene, isobutane, *n*-butane, butene-1, isobutene, *trans*- and *cis*-butene-2 and butadiene, in that order.

Columns A and B, internal to the chromatographic unit, were held at $T = 112$°C, while column C, external, was operated at room temperature. Analysis was carried out in such a way that the carrier gas purges a sample into columns A, B, and C, inserted in series. Separation occurs in this

order: after trapping gases in column C, liquids are analyzed by purging columns B and A; finally, gases are eluted from column C and analyzed. Overall propylene conversion was calculated from peak areas in the feed and in the effluent. Yields to various products were estimated from ratios of peak areas corrected for stoichiometric and chromatographic factors versus propylene in the feed. Selectivities to various products were accounted for on the basis of the sum of yields to various products. The difference between the overall propylene conversion and the sum of the yields to various products represented the percentage of reactant chemisorbed or coked.

RESULTS

Pulse experiments. Figure 1 shows the variation in the overall catalytic activity as a function of the composition: curve (a) refers to results over dehydrated catalysts

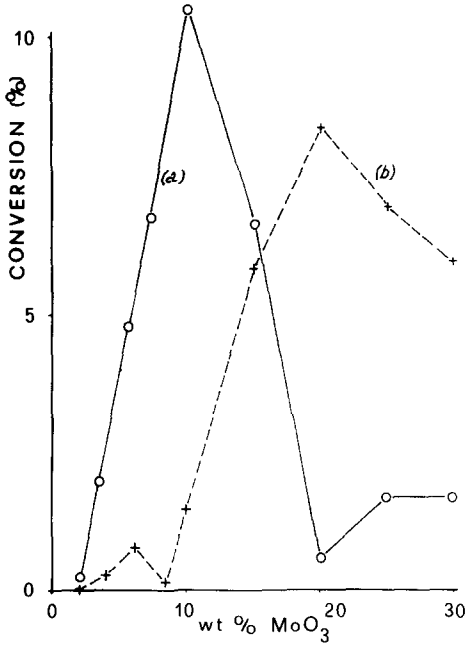

FIG. 1. Conversion of propylene at 300°C, expressed as total sum of yields to various products, as a function of catalyst composition: curve (a), runs in the absence of water (Mode 1); curve (b), runs in the presence of water (Mode 2).

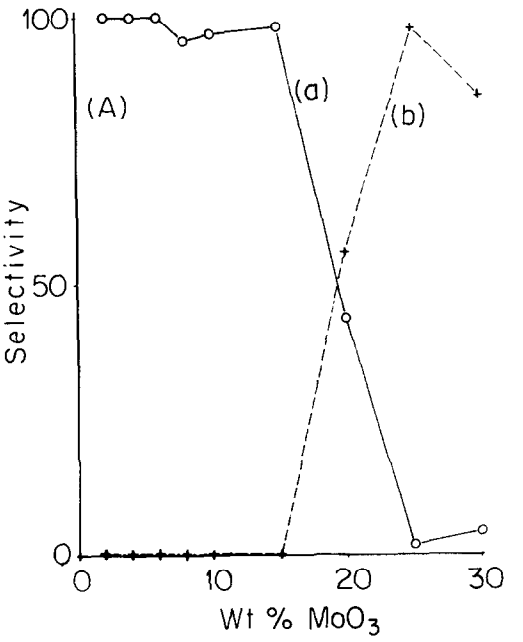

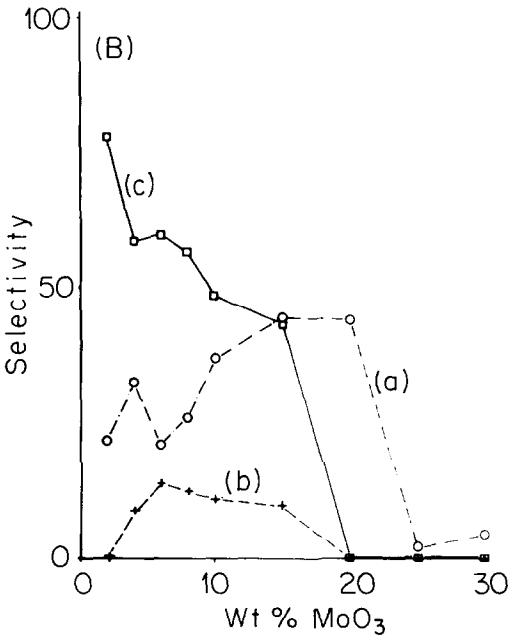

FIG. 2A. Product distribution for runs in the absence of water (Mode 1): (a) summary of selectivities to products of disproportionation, (b) selectivity to acetone. (B) Selectivities to products of disproportionation: (a) ethylene; (b) butene-1; (c) *cis*- and *trans*-butene-2. Runs in the absence of water (Mode 1).

(Mode 1), curve (b) to results over catalysts tested according to Mode 2. The comparison clearly indicates that the overall reaction is strictly governed by the presence of water which causes poisoning of catalytic activity in the low MoO_3 region and enhancement at higher MoO_3 compositions (curve b); instead, in the absence of water the highest activity is found in the low MoO_3 region (curve a). Details of the catalytic performance are further illustrated in Fig. 2A in terms of selectivity for experiments in the absence of water (Mode 1); results clearly indicate again an entirely different course of the reaction depending upon the catalyst composition with disproportionation accounting for the low MoO_3 region (curve a in Fig. 2A), while acetone is the main reaction product on the high MoO_3 side (curve b). Product distribution in the disproportionation region comprises ethylene, butene-1, *cis*- and *trans*-butene-2, as shown in Fig. 2B for the first pulse. Closer appraisal of results indicates, at least for the samples up to MoO_3-15, compliance of the butene-1 percentage and the *trans*- to *cis*-butene-2 ratio to that expected on the basis of thermodynamic data (*7*): for instance, compare the observed 13–18% of butene-1 with the expected 14% and the 1.3–1.6 *trans*/*cis* ratio with the theoretical value of 1.70. Results for the MoO_3-2 sample are out of order, possibly because of the inaccuracy due to the overall activity.

A quite similar behavior was observed in the experiments carried out in the presence of water (Mode 2) which causes, as already discussed, a lowering of catalytic activity in the low MoO_3 region. Details of this behavior are given elsewhere (*6*) in connection with acetone formation.

Tail experiments. Results presented in Table 1 clearly indicate the importance of careful conditioning upon catalytic activity: optimal conversion is in fact obtained only after a prereduction step (1 hr at

TABLE 1

INTENSITIES OF ELECTRONIC SPECTRA AND EPR SPECTRA OF MoO_3-10-500 AS A FUNCTION OF INCREASING SEVERITY OF TREATMENT[a]

Sample	Treatment	Catalytic activity	Absorbances in reflectance spectra (nm)								EF
			270	330	400	500	680	1000	Max uv	Max visible	I(g
1	Drying 15 hr/110°C	—	0.99	0.73	0.14	0.04	0.03	0.04	280	—	Abs
2	Outgassing 2 hr/540°C	—	1.01	0.91	0.68	0.62	0.45	0.32	300	400 sh	24
3	Outgassing 2 hr/540°C Disproportionation 100°C	0	0.95	0.88	0.69	0.64	0.47	0.29	295	450	28
4	Outgassing 15 hr/540°C Disproportionation 100°C	2.2%	0.96	0.86	0.69	0.64	0.44	0.28	280 pl	400 sh	25
5	Outgassing 2 hr/540°C Reduction 1 hr/540°C	—	1.04	1.11	1.00	0.90	0.70	0.54	320	400 sh	43
6	Outgassing 2 hr/540°C Reduction 1 hr/540°C Disproportionation 100°C	35.7%	1.06	1.18	1.04	0.97	0.82	0.62	325	400 sh	6:

[a] sh = shoulder; pl = plateau.

540°C with CO) is included in the sequence. The observation is not new, as it has often been stated in previous literature (*8,9*); however, more emphasis is now added to it through the results obtained from diffuse reflectance spectra, as given in Fig. 3. Increasing severity of pretreatment leads to enhancement of the absorbance in the uv and visible region, thus indicating increase of molybdenum-reduced species on the surface. Closer appraisal of spectra indicates that the whole region up to 1000 nm is involved, with the most striking variations at higher λ. As to the nature of specific configurations reflecting the observed shifts, reference should be made to the literature (*10–17*) and to our previous papers (*4,5*) for more details. To facilitate the discussion, some spectral positions have been singled out from Fig. 3 and their intensities are reported in Table 1 in comparison with catalytic activity. Selected positions include (a) the 270 nm band pertaining to tetrahedral Mo(VI) (*10–12*), (b) the 330 nm band which characterizes octahedral Mo(VI) (*10–12*), but indicates, in combination with the 270, 400 and 500 nm bands, bis-molybdenyl-like structures with dimeric Mo(V) as in the $Mo_2^{V}O_3(acac)_4$ complex (*13, 14*), (c) the characteristic 400–450 nm band of Mo(V) in C_{4v} or O_h coordination (*10, 12*), (d) the 500 nm band attributable to either Mo(IV) (*15*) or to tetrahedral Mo(V) (*12,16*), and (e) the 680 (600–700) nm band due to Mo(V) as in $Mo_4O_{10}(OH)_2$ or reduced heteropolyacids, with Mo(V) in square pyramidal coordination (*16,17*). Besides the recorded frequencies, it is instructive to consider the 800–1200 nm region attributed by Asmolov and Krylov (*12*) to transitions of Mo(V) in tetrahedral coordination. From comparison of these spectral data with catalytic activity (Table 1), it emerges that active catalysts must possess some specific reduced molybdenum

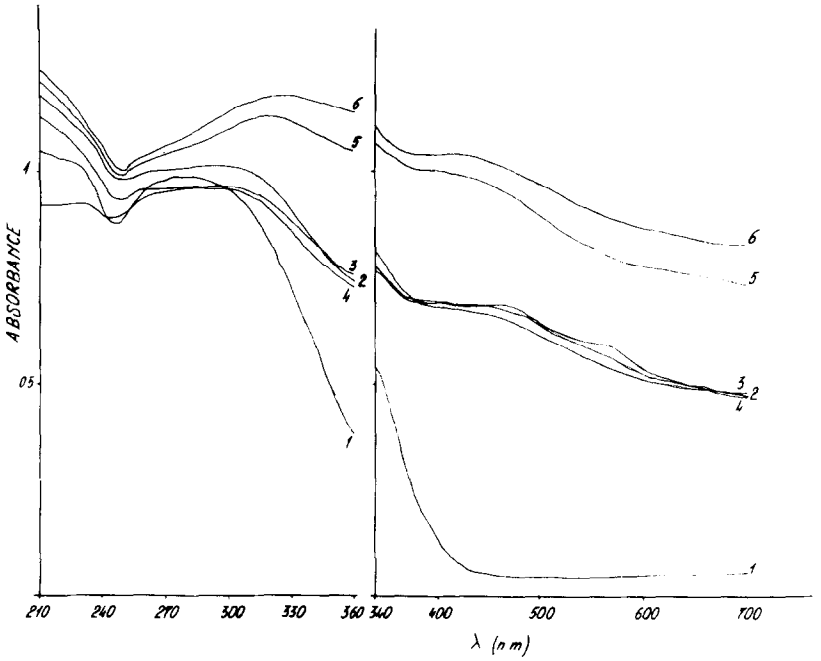

FIG. 3. Optical reflectance spectra of MoO_3-10-500 samples after drying at 110°C (1), outgassing at 540°C for 2 hr (2), outgassing at 540°C for 2 hr and disproportionation at 100°C (3), outgassing at 540°C for 15 hr and disproportionation at 100°C (4), outgassing (2 hr) and reduction (1 hr) at 540°C (5), outgassing (2 hr) and reduction (1 hr) at 540°C followed by disproportionation at 100°C (6).

species. To explain the required specificity, let us consider more closely Fig. 3 and Table 1: samples 2 and 3, although they contain reduced species (note the increase of the 400 and 500 nm bands) are completely inactive. Slight modifications induced by more prolonged time of outgassing (15 hr) cause weak catalytic activity (sample 4). High disproportionation rates are displayed by the reduced samples 5 and 6, both characterized by enhanced absorption in the 320–330 nm region and by further increase, with respect to the outgassed samples, of the 400 nm and 500 nm bands. Altogether it appears that catalytic activity is specific to surface species displaying the 330, 400 and 500 nm absorption bands in combination with the unchanged 270 nm band: as all these positions are shared by bis-molybdenyl-like structures (*5,13,14*) these are most likely to be responsible for catalytic activity.

In order to collect further evidence for the assignment made above, a relationship was sought between the time of CO reduction and catalytic activity, at 100°C. Results of these experiments are given in Fig. 4 for the overall conversion and selectivities and in Fig. 5 for the EPR and diffuse reflectance intensities. The results clearly indicate an adverse effect of time of reduction upon catalytic activity. Lowest activities are in fact displayed by "activated" or low-reduced samples, as well as by catalysts reduced for more prolonged times (> 180 min). Maximum activity occurs within a broad interval of reduction times, i.e., from 60 to 180 min. The material balance was of the order of 99% or better, except for the 240 min experiment, for which extensive cracking was found to occur. Consequently, the accuracy of the

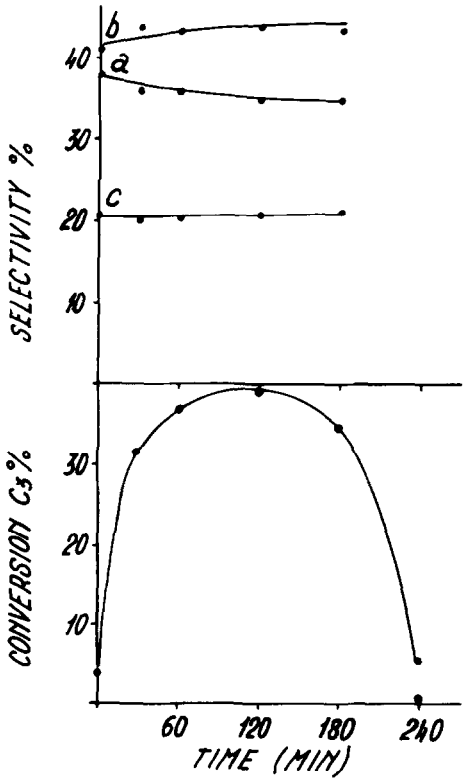

FIG. 4. Conversion of propylene and selectivities to products of disproportionation at 100°C: (a) ethylene, (b) *trans*-butene-2, (c) *cis*-butene-2, vs reduction time (on weight basis).

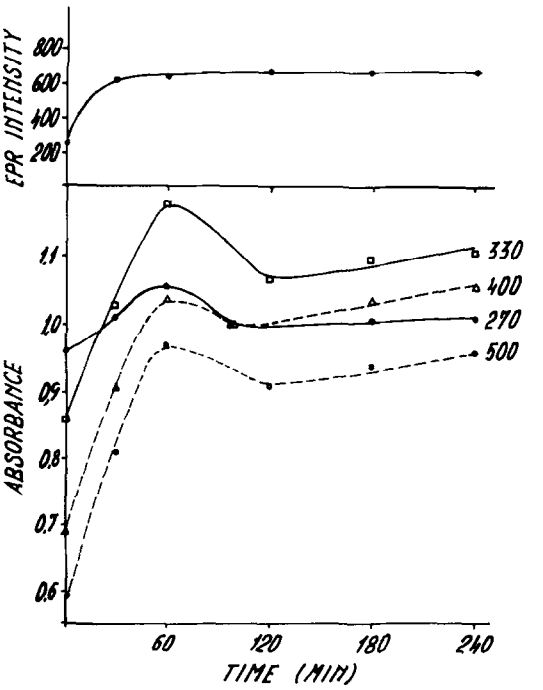

FIG. 5. Variation of Mo(V) EPR signal intensity and of some characteristic optical reflectance absorption intensities as a function of the time of reduction.

selectivities was low and they were therefore omitted in Fig. 4. In all other experiments (0–180 min reduction) the product distribution follows the stoichiometric 1:1 ethylene/butenes ratio. The absence of butene-1 complies well with information (*8,9*) indicating that prereduction causes a decrease in double-bond isomerization and also indicates that butene-2 is a primary reaction product. As to the *trans/cis* ratio of 2.3 at 100°C, the agreement between experimental and calculated values proves that the reaction is not influenced by the reduction state of the catalysts.

With regard to the possible active reduced molybdenum species, we note that (a) the EPR intensities first increase with the time of reduction and then level off to constant values, at 60 min (b) the intensities of all diagnostic absorptions in the electronic spectra show a sharp maximum at 60 min reduction time and afterwards decrease; further increase in reduction times leads to bending of intensities upwards although at a slightly different pace (500 > 400 > 300 > 270 nm).

To sum up, it appears that (a) monomeric Mo(V) species, responsible for the EPR spectra (and for the 400 nm absorption band), do not properly describe the catalytic behavior; (b) the maximum in the disproportionation activity is better related to the presence of bis-molybdenyl-like species, at least for reduction times of the order of 60–120 min; (c) enhanced formation of monomeric Mo(V) (400 nm) and of Mo(IV) (500 nm) at higher reduction times (> 120 min) appears to have an adverse effect upon catalytic activity, thus providing additional support to the observations under b.

To elucidate these aspects further, a series of experiments was performed in the range 50–200°C, at otherwise constant conditions of pretreatment (60 min reduction by CO). Results in terms of end-point conversion (see below) are plotted in Fig. 6: it shows a volcano-shaped curve with a well-defined maximum between 100 and 150°C, in good agreement with previous findings on similar systems (*8,9*). Within this region of temperature, conversion was found to be constant with time on stream, in contrast to runs at other temperatures, the end-point conversions (Fig. 6) of which were found to decay as following: 7.1, 4.3 and 2.1% at 50°C; 38, 27 and 24% at 200°C, respectively, after 1, 2 and 3 hr on stream. As to the product distribution, butene-1 was always lower than expected from thermodynamics (*7*), also in accordance with literature (*8,9*) and previous findings (Fig. 4). The *trans/cis* ratios were close to the calculated values (*7*) except for runs at 50°C. The lower ratio and lower conversion at this temperature can

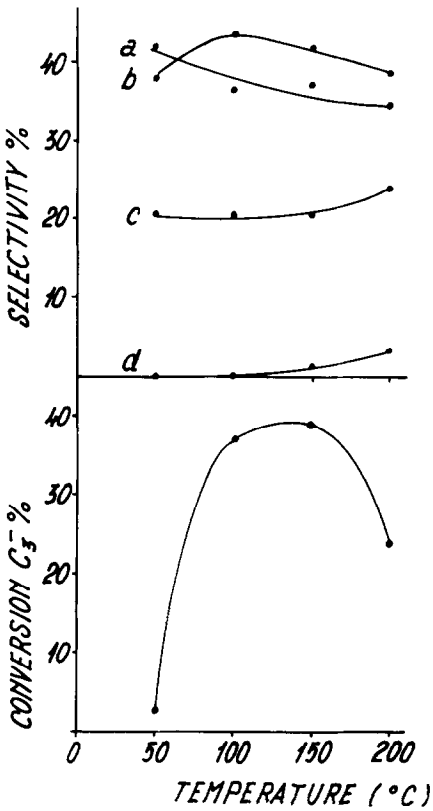

FIG. 6. Variations of conversion of propylene and selectivities to products of disproportionation: (a) ethylene, (b) *trans*-butene-2, (c) *cis*-butene-2, (d) butene-1, as a function of the reaction temperature (on weight basis).

be attributed to kinetic control. On the other hand, at $T > 150$°C the lower conversions can find a reasonable explanation, analogous to that given in similar systems (*8,9,18,19*), namely by mass-transfer control (*18*) or by reversible deactivation of sites superimposed on the irreversible poisoning of sites (*19*). In addition, the present results show that decay of catalytic activity at high T may be related to specific properties of the solid. The conclusion is arrived at by comparing Figs. 6 and 7. Maximum activity at 100–150°C appears to be related to a specific nature of the reduced molybdenum species similar to that found as a function of the reduction time (Fig. 5). Moreover, the bending upwards of the absorption bands of monomeric Mo(V) (400 nm) and of Mo(IV) (500 nm) at increasing T (Fig. 7) indicates that formation of these species occurs more rapidly than that of the bis-molybdenyl-like structure: decay of catalytic activity at higher T may thus be understood on this basis. Further support for these conclusions is implicit in the lack of correspondence between catalytic activity and EPR intensities (Fig. 7).

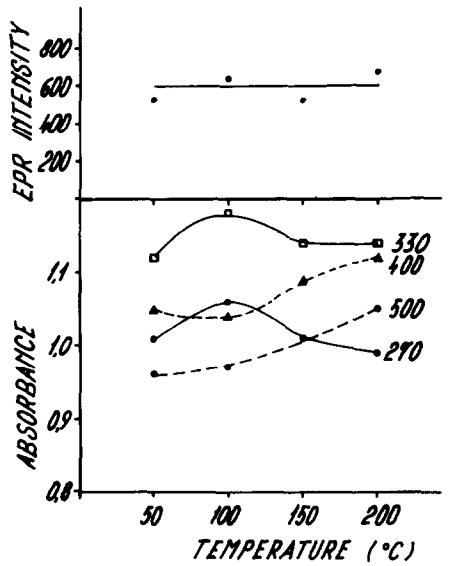

FIG. 7. Variation of Mo(V) EPR signal intensity and of characteristic optical absorption intensities as a function of the reaction temperature.

DISCUSSION

Results of catalytic activity (Fig. 1) prove undoubtedly the existence of two distinct regions in the $MoO_3 \cdot Al_2O_3$ system: disproportionation activity in the low MoO_3 region (up to 10–15 wt% MoO_3) and oxyhydration to acetone in the high MoO_3 region (from MoO_3-15 upwards). A first correlation with solid state properties may be derived from the observation of close correspondence between the twin peak distribution of the Mo(V) signal [Fig. 3 of Part II (*5*)] and catalytic activity (Fig. 1). On this basis, one is entitled to assign a definite role to Mo(V) in both reactions. A precise definition of this role and all related aspects are discussed here for the disproportionation activity; in Part IV (*6*) we consider in detail acetone formation.

Results of Figs. 4–7, indicating lack of dependency of catalytic activity upon the EPR signal intensities, suggest that the statement of Mo(V) (*20,21*) being the active site needs further refinement. The apparent contradiction with previous results is removed by considering the electronic spectra of used catalysts: thus while the presence of Mo(V) is still confirmed (see the 400 and the 500 nm bands), the simultaneous increase of absorption at 330 nm on the most active catalysts suggests the presence of Mo(V) in a more complex configuration, i.e., as in bis-molybdenyl-like species containing Mo(V) pairs in a $[OMo{-}O{-}MoO]^{4+}$ structure (*13,14*). On this basis, it seems reasonable to correlate catalytic activity with the 270 nm and 330 nm bands, as these bands only account properly for the species; in contrast, the 400 and 500 nm bands, in common with simpler Mo(V) configurations (i.e., monomeric species) as well as with Mo(IV), should be considered as pertaining to

structures accompanying bis-molybdenyl but not relevant to the catalytic activity. More evidence for this is that the decay of catalytic activity following increasing time of reduction (Fig. 4) or temperature (Fig. 6) is accompanied by an adverse course of the 270–330 nm vs the 400–500 nm bands (Figs. 5 and 7): thus, while the former more closely follow the catalytic activity, the latter vary antibatically, i.e., increase with decreasing catalytic activity. The observed behavior of the 400–500 nm bands can be readily understood: namely, more extreme conditions (increasing time of reduction T of reaction) are expected to favor a higher population of monomeric Mo(V) and formation of more reduced species, i.e., Mo(IV), in accordance with previous observations (*22*). The result further strengthens our belief in bis-molybdenyl-like active sites and explains lack of correlation with EPR intensities.

As disproportionation activity has been reported over a wide variety of catalysts (*8,9*) differing considerably in the valence state of molybdenum [compare $Mo(CO)_6$ and $MoO_3 \cdot Al_2O_3$], it could appear that the oxidation state of Mo is not the key factor in determining the reaction course. This image of the catalysts should now be revised, following present findings and the most recent results of Howe *et al.* (*23*) and Davie *et al.* (*24*) on $Mo(CO)_6$ and of Henrici-Olivé and Olivé (*20*) and Nakamura *et al.* (*21*) on $MoO_3 \cdot Al_2O_3$: accordingly, molybdenum species with lower than maximum valence state are said to play a primary role in determining catalytic activity. Further proof in favor of reduced Mo states may be inferred from most patent and technical literature, which indicate enhancement of activity and selectivity by a controlled treatment with reducing gases after calcination. In this context, the well-known poisoning effect of polar molecules such as water is interpreted in terms of strong chemisorption into the empty coordination sphere of unsaturated Mo ions (σ-type bonds), in competition with the olefin.

On the basis of the foregoing, a reaction scheme can now be proposed that involves primarily π-type bonding of the olefin to Mo(V), implying bis-molybdenyl-like dimeric Mo(V) species. Although details of the stereochemistry of the reaction cannot be given at present, it is proposed on the assumption of the square pyramidal configuration of the model compound and the preferred coordination number of six, that reaction is initiated through olefins coordinating to two neighboring Mo(V) positions with formation of a four-center complex as already postulated (*8,9*), changing the Mo(V) geometry from C_{4v} to O_h. Desorption is expected to occur with breakage of two opposite bonds without hydrogen shift. Kinetic information from the literature further supports this viewpoint: thus while a number of possible mechanisms have been considered, only the dual site mechanism has proven successful in correlating experimental data: this interpretation is favored by Lewis and Wills (*25*) and by Moffat and Clark (*26*) for cobalt molybdate, by Davie *et al.* (*27*) for supported $Mo(CO)_6$, and by Banks and Bailey (*19*) for MoO_3 on Al_2O_3.

CONCLUSIONS

The variations in overall catalytic activity of $MoO_3 \cdot \gamma\text{-}Al_2O_3$ as a function of the composition, studied for propylene in pulse and tail experiments, indicate the importance of careful conditioning of the samples by prereduction and the absence of water during the reaction. Correlation of catalytic activity with previous studies on the surface structure of oxidized and reduced catalysts and a study of the optical reflectance spectra of variously conditioned samples indicates the active role of a specific reduced molybdenum species with a bis-molybdenyl structure, thus containing a Mo(V) pair. On the contrary,

monomeric Mo(V) species, detectable by EPR, and arising from drastic reduction together with Mo(IV), do not properly describe the catalytic activity.

REFERENCES

1. John, G. S., Den Herder, M. J., Mikovsky, R. J., and Waters, R. F., *in* "Advances in Catalysis" (D. D. Eley, W. G. Frankenburg, V. I. Komarewsky and P. B. Weisz, Eds.), Vol. 9, p. 252. Academic Press, New York, 1957.
2. Seshadri, K. S., and Petrakis, L., *J. Phys. Chem.* **74,** 4102 (1970).
3. Boreskov, G. K., Dzis'ko, V. A., Emel'yanova, V. M., Pecherskaya, Y. I., and Kazanskii, V. B., *Dokl. Akad. Nauk SSSR* **150,** 829 (1963).
4. Giordano, N., Bart, J. C. J., Vaghi, A., Castellan, A., and Martinotti, G., *J. Catal.* **36,** 81 (1975).
5. Giordano, N., Castellan, A., Bart, J. C. J., Vaghi, A., and Campadelli, F., *J. Catal.* **37,** 204 (1975).
6. Giordano, N., Vaghi, A., Bart, J. C. J., and Castellan, A., *J. Catal.* **38,** 11 (1975).
7. Condon, F. E., *in* "Catalysis" (P. H. Emmett, Ed.), Vol. 6, p.43. Reinhold, New York, 1958.
8. Bailey, G. C., *Catal. Rev.* **3,** 37 (1969).
9. Banks, R. L., *Fortschr. Chem. Forsch.* **25,** 39 (1972).
10. Asmolov, G. N., and Krylov, O. V., *Kinet. Katal.* **11,** 1028 (1970).
11. Ashley, J. H., and Mitchell, P. C. H., *J. Chem. Soc. A* 2821 (1968).
12. Asmolov, G. N., and Krylov, O. V., *Kinet. Katal.* **13,** 188 (1972).
13. Larson, M. L., and Moore, F. W., *Inorg. Chem.* **2,** 881 (1963).
14. Gebrke, H., and Veal, J., *Inorg. Chim. Acta* **3-4,** 623 (1969).
15. Porter, V. R., White, W. B., and Roy, R., *J. Solid State Chem.* **4,** 250 (1972).
16. Mitchell, P. C. H., and Trifirò, F., *J. Chem. Soc. A* 3183 (1970).
17. Papaconstantinou, E., and Pope, M. T., *Inorg. Chem.* **9,** 667 (1970).
18. Moffat, A. J., Clark, A., and Johnson, M. M., *J. Catal.* **22,** 379 (1971).
19. Banks, R. L., and Bailey, G. C., *Ind. Eng. Chem. Prod. Res. Develop.* **3,** 170 (1964).
20. Henrici-Olivé, G., and Olivé, S., *Angew. Chem.* **85,** 148 (1973).
21. Nakamura, R., Morita, Y., and Echigoya, E., *Nippon Kagaku Kaishi* **2,** 244 (1973).
22. Seshadri, K. S., and Petrakis, L., *J. Catal.* **30,** 199 (1973).
23. Howe, R. F., Davidson, D. E., and Whan, D. A., *J. Chem. Soc. Faraday Trans.* **1,** 68, 2266 (1972).
24. Davie, E. S., Whan, D. A., and Kemball, C., *Chem. Commun.* 1430 (1969).
25. Lewis, M. J., and Wills, G. B., *J. Catal.* **15,** 140 (1969).
26. Moffat, A. J., and Clark, A., *J. Catal.* **17,** 264 (1970).
27. Davie, E. S., Whan, D. A., and Kemball, C., *J. Catal.* **24,** 272(1972).